Ion Thruster Facility Effects Characterization via Computational Analysis

IEPC-2022-264

Presented at the 37th International Electric Propulsion Conference
Massachusetts Institute of Technology, Cambridge, MA, USA
June 19-23, 2022

Richard A. Obenchain[1] and Richard E. Wirz[2], AIAA Associate Fellow
University of California, Los Angeles, CA, 90095, USA

The effects of neutral ingestion on gridded ion thruster operation due to background pressure in the test facility have not been studied in detail. We propose a new quantity, the ingestion factor, as the ratio of environmental flux to thruster flux. Using the ingestion factor and the NSTAR TH15 configuration, we modeled neutral ingestion as a change to the neutral transparency of the grid for a range of background pressures (10^{-7} Torr to 10^{-4} Torr). Beam current density and beam power showed discernible variation in the model, even at the pressure recommended pressure for thruster testing (10^{-5}). We then propose adjusting the plenum flow by a scaled ingestion factor for the simulated-ingestion cases as a method of approximating true vacuum operation. Two specific scaling factors were tested, with both showing desirable effect on the beam characteristics. Future work will include validation and further refinement of the specific equations.

I. Introduction

The role of facility effects in ground-based thruster testing is one of the most important ongoing discussions in the electric propulsion community[1–6]. These effects can be described as the changes in thruster operation caused by environmental characteristics that differ between a ground-based testing facility and a thruster's intended operational environment in space. As part of the efforts of Joint AdvaNced PropUlsion InStitute (JANUS) funded by NASA, Predictive Engineering Models (PEMs) are being developed to analyze thruster operation during ground testing, account for uncertainty due to various parameters including facility effects, and extrapolate to predict in-flight operation and operational lifetime[1].

Ingestion of ambient neutral gas into the thruster is one area of concern. In the PEM framework (Fig. 1), ingestion constitutes a coupling of thruster (H_T) and environment (H_E) studies as part of predicting thruster performance. With generally higher propellant flow rates and thus increased concerns regarding facility background pressure, the effects of neutral ingestion on Hall effect thrusters (HETs) have been subject to numerous investigations in recent years[7–10]. Research on the effects of ingestion on gridded ion thrusters (GITs) has been limited; however, efforts to increase power and thrust of GITs for future missions will need additional modeling and support to understand the role of neutral ingestion on GIT performance characteristics.

We present an approach for modeling thruster operation in the presence of a background pressure as a modification of grid neutral transparency and example . We propose an ingestion factor useful in understanding the rate of ingestion relative to thruster operation. A best-in-class discharge chamber model is employed to observe the relative changes induced by modification of neutral transparency. We then propose a basic model for modifying the thruster's propellant flow in a way targeted to mimic true vacuum (in-flight) operation and compare the modified thruster operation to prior cases.

[1]PhD. Student, Mechanical and Aerospace Engineering, robenchain@g.ucla.edu, AIAA Student Member
[2]Professor, Mechanical and Aerospace Engineering, wirz@ucla.edu

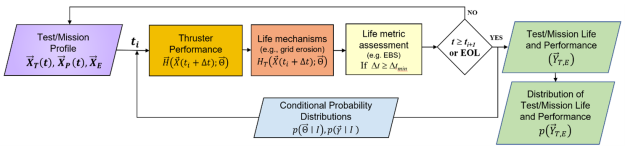

Fig. 1 The Predictive Engineering Model's iterative framework[1].

II. Modeling Ingestion

[Fluff] We start by considering an ion thruster in simplified terms as composed of three primary features: the interior of the thruster, the external environment, and some boundary that denotes the transition between the two. For any ion thruster (and indeed any propellant-based propulsion system) to provide thrust, there must be a flux of material from the interior of the thruster to the boundary, with some portion of that flux (between 0% and 100%) passing through the boundary to the environment. We label this flux from the interior of the thruster to the boundary as Γ_t. Likewise, there may be a flux from the environment to the boundary, with some portion of that flux also passing through to the interior of the thruster. We label this environmental flux to the boundary as Γ_{env}.

Ingestion can be defined as the transfer of matter in the environment to the interior the thruster. The rate of ingestion is proportional to the flux to the boundary, that is, to Γ_{env}. In most cases, the relevance of Γ_{env} will depend on its magnitude relative to Γ_t. We define the ratio of these two fluxes as the ingestion factor λ_i:

$$\lambda_i \equiv \frac{\Gamma_{env}}{\Gamma_t}, \text{ ingestion factor} \tag{1}$$

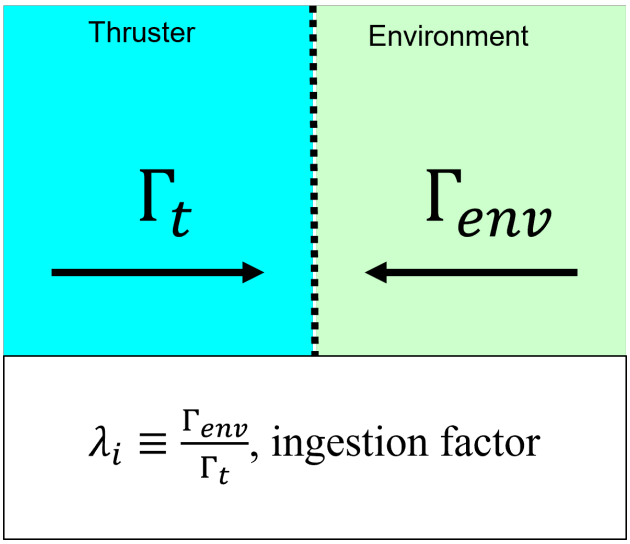

Fig. 2 The ingestion factor λ_i is defined as the ratio of the flux from the environment to the flux from the thruster.

In thruster terms, the ingestion factor represents the rate at which particles enter the thruster from the environment relative to the rate at which particles leave the thruster. This has relevance to a number of situations, of which thruster operation in a vacuum chamber is only one. For example, use of a thruster in rarefied but nonzero atmospheric conditions, such as in Very Low Earth Orbit or in debris fields (such as planetary rings) around other bodies, would likely lead to ingestion and thus $\lambda_i \neq 0$.

For thruster operation within a facility, Γ_{env} will depend primarily on the presence of background gas within the vacuum chamber. Exact calculation of Γ_{env} is complicated, as the exact geometric and thermal characteristics of the chamber as well as operation of the thruster will impact the neutral density near the thruster boundary. The simplified thermal flux model implemented here is commonly used and considered a reasonable approximation in most studies.

In contrast, calculation of Γ_t is generally simpler, as the local characteristics of the thruster itself dominate the region. The physical structure of the thruster determines the boundary between thruster and environment; for GITs, the

grid(s) are almost always considered to be the boundary, with the discharge chamber representing the internal thruster environment; for HETs, the plane of the channel exit is the reasonable choice. Figure 3 presents a visual representation of these boundaries and the subsequent calculation of λ_i.

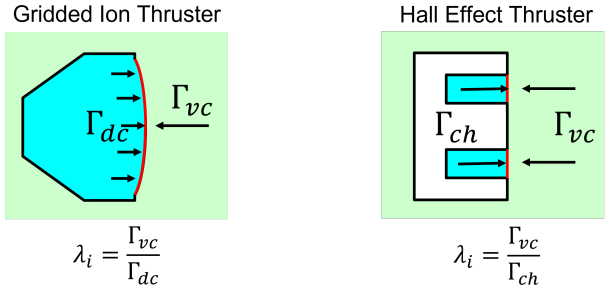

Fig. 3 Calculation of the ingestion factor λ_i will vary between thruster designs and operational environments.

The ingestion factor λ_i is inherently present in multiple aspects of modeling ingestion. Exact application to the current model will be shown later.

A. General Flow Equations

The standard unit of measurement for pressure within a vacuum chamber is the Torr, with typical vacuum chambers for thruster testing operating in the range of 10^{-9} Torr to 5^{-4} Torr. Conversion from Torr to Pascal (Pa) is trivially accomplished with a multiplicative factor of 133.32 Pa/Torr.

It is generally more convenient to refer to particle density n (particles per cubic meter, often simply written as m^{-3}) during calculations. For the specific conversion between P (in Torr) and n (in #/m^2), please refer to the Appendix.

For this analysis, we assume all gas in the discharge chamber and vacuum environment is xenon. Therefore, we refer to $\dot{m}$ throughout this work interchangeably between units of #/s (when referring to particle flow in early sections) and kg/s (when referring to fuel flow in later sections).

A GIT within a vacuum chamber will experience a flow of neutral gas particles from the chamber to (and partly through) the thruster's grid. The neutral particle flow to the outer surface of the grid can be described as:

$$\dot{m}_{grid,env} = \Gamma_{env} A_{grid} \tag{2}$$

... where Γ_{env} is the particle flux from the vacuum chamber environment to the grid and A_{grid} is the area of the grid. The exact determination of Γ_{env} can be complex; however, in a simple thermal model, we calculate Γ_{env} as:

$$\Gamma_{env} = \frac{n_{env}\bar{c}_{env}}{4} = \frac{n_{env}}{4}\sqrt{\frac{2kT_{env}}{\pi m}} = \frac{n_{env}\sqrt{kT_{env}}}{\sqrt{8\pi m}} \tag{3}$$

... where n_{env} is the neutral density within the vacuum chamber, $\bar{c}_{env}$ is the mean velocity of neutrals within the vacuum chamber, k is Boltzmann's constant, T_{env} is the neutral temperature within the vacuum chamber, and m is the mass of a single neutral atom. Substituting Eq. (3) into Eq. (2), we have:

$$\dot{m}_{grid,env} = \frac{A_{grid} n_{env}\sqrt{kT_{env}}}{\sqrt{8\pi m}} \tag{4}$$

Ingestion of neutrals from the vacuum chamber into the discharge chamber takes place through the grid and is determined by grid transparency ϕ. This ingestion can be generalized as:

$$\dot{m}_{in,env} = \dot{m}_{grid,env}\phi = \frac{A_{grid}\phi n_{env}\sqrt{kT_{env}}}{\sqrt{8\pi m}} \tag{5}$$

... where $\dot{m}_{in,env}$ is the particle flow into the discharge chamber from the vacuum chamber.

We can similarly define the particle flow of neutrals from the discharge chamber to the grid as:

$$\dot{m}_{grid,t} = \Gamma_{out,t} A_{grid} \tag{6}$$

Γ_{out_t} is the neutral particle flux per unit area from the discharge chamber. We can likewise use thermal flux to approximate Γ_{out_t} as:

$$\Gamma_{env} = \frac{n_t \bar{c}_t}{4} = \frac{n_t}{4}\sqrt{\frac{2kT_t}{\pi m}} = \frac{n_t\sqrt{kT_t}}{\sqrt{8\pi m}} \tag{7}$$

... where n_t is the neutral density within the discharge chamber, $\bar{c}_t$ is the mean velocity of neutrals within the discharge chamber, k is Boltzmann's constant, and T_t is the neutral temperature within the vacuum chamber*. The most relevant values for n_t and T_t are those adjacent to the grid; we will discuss some implications of this later.

Substituting Eq. (7) into Eq. (6), we get:

$$\dot{m}_{grid,t} = \frac{A_{grid} n_t \sqrt{kT_t}}{\sqrt{8\pi m}} \tag{8}$$

The neutral particle flow from the discharge chamber through the grid can then be determined as the portion of $\dot{m}_{grid,t}$ that passes through the grid of given transparency ϕ. Thus:

$$\dot{m}_{out,t} = \phi \dot{m}_{grid,t} = \frac{A_{grid}\phi n_t \sqrt{kT_t}}{\sqrt{8\pi m}} \tag{9}$$

Equation (9) mirrors Eq. (9).

From the perspective of the discharge chamber, the flow in through the grid from the vacuum chamber is considered ingestion:

$$\dot{m}_{ingested,t} = \dot{m}_{in,env} = \dot{m}_{grid,env}\phi \tag{10}$$

We can also describe the neutral particle flow reflected from grid back into the discharge chamber as:

$$\dot{m}_{reflected,t} = (1-\phi)\dot{m}_{grid,t} = \frac{A_{grid}(1-\phi) n_t \sqrt{kT_t}}{\sqrt{8\pi m}} \tag{11}$$

B. Pseudo-Transparency

Let us consider two scenarios.

In the first scenario, the thruster is operating within a vacuum chamber with a nonzero pressure, resulting in ingestion of gas into the discharge chamber. Within the discharge chamber, the flow of neutrals into the discharge chamber from the grid is thus the sum of the reflected and ingested neutral flows.

$$\dot{m}_{in,t,a} = \dot{m}_{reflected,t,a} + \dot{m}_{ingested,t,a} \tag{12}$$

Substituting in Eqs. (11) and (10), we get:

$$\dot{m}_{in,t,a} = (1-\phi)\dot{m}_{grid,t,a} + \dot{m}_{grid,env,a}\phi \tag{13}$$

In the second scenario, the thruster is considered to be operating in a true vacuum. In this case, there is no ingestion, and the flow of neutrals into the discharge chamber from the grid is simply the neutral flow reflected from the grid:

$$\dot{m}_{in,t,b} = (1-\phi_p)\dot{m}_{grid,t,b} \tag{14}$$

It is possible to have these two scenarios experience equal $\dot{m}_{in,t}$. That is to say, there are values of ϕ_b and $\dot{m}_{grid,t,b}$ for which the neutral flow as experienced by the discharge chamber is equal to that in Scenario 1. Mathematically:

$$\dot{m}_{in,t,a} = \dot{m}_{in,t,b} \tag{15}$$

$$(1-\phi)\dot{m}_{grid,t,a} + \dot{m}_{grid,env,a}\phi = (1-\phi_p)\dot{m}_{grid,t,b} \tag{16}$$

*The subscript t is used here to indicate neutrals from the thruster; the use of o,t for neutrals from the thruster would be more consistent with convention, but the assumption is that all mass and particle quantities here relate to neutrals unless explicitly stated otherwise

We further state that these two scenarios (a) and (b) are starting from the same initial state; that is, that $n_{t,a} \cong n_{t,b}$ and thus the neutral flows to the grid are approximately equal ($\dot{m}_{grid,t,a} \cong \dot{m}_{grid,t,b}$). This allows us to restate Eq. (16) as:

$$(1-\phi)\dot{m}_{grid,t} + \dot{m}_{grid,env,a}\phi = (1-\phi_p)\dot{m}_{grid,t} \tag{17}$$

This relation tells us that, for some real transparency ϕ_a (going forward referred to simply as ϕ, there is a **pseudo-transparency** ϕ_p that can reproduce the same $\dot{m}_{in,t}$ without ingestion (e.g., while operating in a true vacuum) at an initial instant. This pseudo-transparency ϕ_p should allow us to model thruster behavior within a vacuum chamber with nonzero background pressure and grid transparency ϕ using a simulation of operation in true vacuum with grid transparency ϕ_p.

C. Deriving the Ingestion Factor and Pseudo-Transparency

Extrapolating further from Eq. (17):

$$\dot{m}_{grid,env}\phi = (1-\phi_p)\dot{m}_{grid,t} - (1-\phi)\dot{m}_{grid,t} \tag{18}$$

$$\dot{m}_{grid,env}\phi = \dot{m}_{grid,t}[(1-\phi_p) - (1-\phi)] \tag{19}$$

$$\dot{m}_{grid,env}\phi = \dot{m}_{grid,t}(\phi - \phi_p) \tag{20}$$

Substituting in from Eqs (4) and (8):

$$\frac{A_{grid}n_{env}\sqrt{kT_{env}}}{\sqrt{8\pi m}}\phi = \frac{A_{grid}n_t\sqrt{kT_t}}{\sqrt{8\pi m}}(\phi - \phi_p) \tag{21}$$

$$n_{env}\sqrt{kT_{env}}\phi = n_t\sqrt{kT_t}(\phi - \phi_p) \tag{22}$$

$$\frac{n_{env}\sqrt{kT_{env}}}{n_t\sqrt{kT_t}} = (1 - \frac{\phi_p}{\phi}) \tag{23}$$

The left-hand side of Eq. (23) represents a critical relationship. Per Eq. (4), $n_{env}\sqrt{T_{env}}$ is proportional to the flux to this boundary from the environment (i.e., the vacuum chamber). Likewise, we see that $n_t\sqrt{kT_t}$ is proportional to the flux to the boundary from the thruster (i.e., the discharge chamber) from Eq. (8). Therefore, we can see that, for this model:

$$\lambda_i = \frac{n_{env}\sqrt{kT_{env}}}{n_t\sqrt{kT_t}} = (1 - \frac{\phi_p}{\phi}) \tag{24}$$

Equation (23) allows us to calculate the pseudo-transparency value ϕ_p from λ_i:

$$\lambda_i = (1 - \frac{\phi_p}{\phi}) \tag{25}$$

$$\phi_p = \phi(1-\lambda_i) \tag{26}$$

With an equation for ϕ_p in hand, we can model a thruster's operation in the presence of varying background pressures.

III. Model: Effects of Ingestion on Beam Characteristics

DC-ION is a hybrid computational model developed with the goal of understanding plasma behavior and characteristics inside the discharge chamber and has been validated against both moderate-power and miniature gridded ion thrusters[11]. The overall model incorporates several sub-models in 2-D and 2.5-D space incorporating both particle-in-cell behavior and general fluid dynamics for a hybrid approach to approximating discharge conditions.

To test the use of λ_i and ϕ_p, we used DC-ION to compute the steady-state operational characteristics of the NASA Solar Technology Application Readiness (NSTAR) thruster under various conditions. NSTAR is a well-documented 28-cm GIT which has been used in space since 1998. The thruster uses xenon as propellant.

Table 1 Relevant operational parameters for the NSTAR thruster TH15.

Grid area	0.0607 m^2
Effective grid transparency	15.61%
Fuel flow	27.15 sccm
–Cathode	3.73 sccm
–Plenum	23.42 sccm

A. Initial Case: Zero ingestion ($\phi_p = \phi$)

As a basis for comparison, we modeled the NSTAR thruster operating at TH15 in a vacuum. The list of parameters relevant for this study are in Table 1.

After completion of model execution, several results needed for further calculations were obtained.

One output of the DC-ION model is the neutral density contour within the discharge chamber (see Fig. **??**). The average neutral density within the discharge chamber is given as a numeric result; for the purposes of neutral flux from the discharge chamber to the grid, the neutral density along the grid is more accurate.

The values for neutral density and temperature along the grid were extracted. As can be seen in Fig. 4, neutral density is lowest along the centerline due to depletion to ions, while neutral density at the outer annulus is highest. These outer annuli constitute more physical area for the grid's surface; an accurate average neutral density along the grid is obtained by weighting according to the surface area of each annulus. Similarly, an average neutral temperature is obtained using the weighted neutral density values for each annulus and averaging across the total neutral count per unit depth.

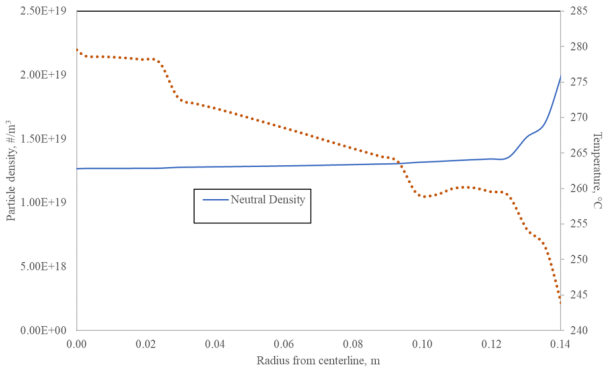

Fig. 4 Neutral density and temperature along the grid for the NSTAR TH15 vacuum operation condition. Data from DC-ION.

The final obtained average neutral density along the grid was $1.37x10_{19}$ #/m_3. The average neutral density for the discharge chamber as a whole was $1.45x10_{19}$ #/m_3; as mentioned, this more general average may be used as an approximation in the absence of grid-specific data. The average temperature along the grid was determined as $261.3°C$ (534.4 K).

B. Operation with Nonzero Ingestion ($\phi_p \neq \phi$)

To model operation within a vacuum chamber with nonzero pressure driving ingestion, five vacuum chamber pressure values were initially chosen as representative of real-world conditions, ranging from 10_{-7} Torr to 10^{-4} Torr. This range was chosen to encompass a sample of facilities and operations; Dankanich et. al recommended that performance testing for GITs be conducted at no greater than $3x10^{-5}$ Torr, suggesting a reasonable maximum upper limit for test conditions of 10^{-4} Torr[12]. During characterisation tests of NASA's Evolutionary Xenon Thruster (NEXT) at NASA Glenn Research Center (GRC), vacuum chamber pressure approximated $3.5x10^{-6}$ Torr, suggesting 10^{-6} Torr as a reasonable lower limit [13]. A further step of 10^{-7} Torr was included in initial calculations as verification of reduced effects at lower pressures; however, these results were indistinguishable from the true vacuum case and dropped. The average temperature of the gas in the vacuum chamber was assumed at approximate room temperature of 300 K. Table 2 has the model parameters

resulting from calculations.

Table 2 Resulting parameters for NSTAR thruster TH15 operation with various vacuum chamber pressures including the defaut case (pressure = 0 Torr).

Pressure Env Torr given	Neutral Density Env n_{env}, #/m^3 Eq. (48)	Ingestion Factor λ_i Eq. (23)	Pseudo-Transparency ϕ_p Eq. (26)
0.00	0.00	0.000%	15.61%
1.00x10^{-7}	3.22x10^{15}	0.018%	15.61%
1.00x10^{-6}	3.22x10^{16}	0.176%	15.58%
1.00x10^{-5}	3.22x10^{17}	1.765%	15.33%
5.00x10^{-5}	1.61x10^{18}	8.824%	14.23%
1.00x10^{-4}	3.22x10^{18}	17.65%	12.86%

As a measure of the variation from the true vacuum case, several beam characteristics were examined. The changes in beam current density profile along the radius are shown on the left in Fig. 5. As the vacuum chamber pressure increases, the beam current density also increases; the growth in beam current is not linear to chamber pressure but does appear to be a constant scaling factor long the grid radius. The changes in total beam power relative to vacuum chamber pressure are plotted on a semilog scale. The profile suggests a nearly-linear growth in beam power with vacuum chamber pressure across the modeled pressure ranges.

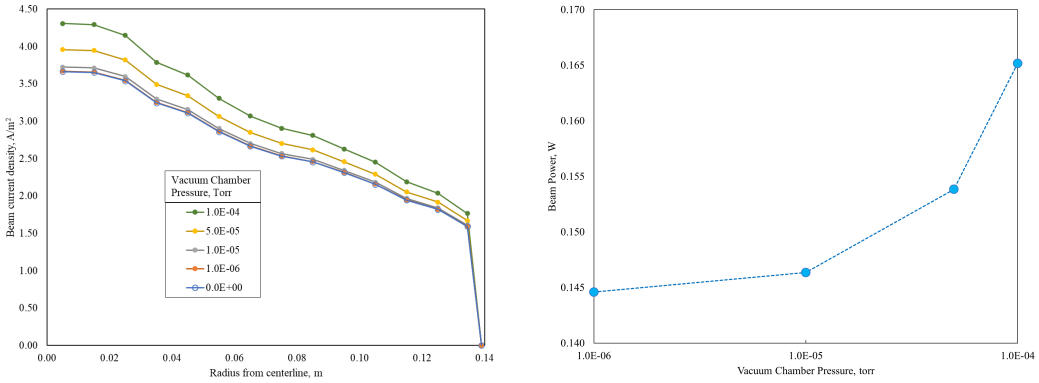

Fig. 5 Left, beam current density along the radius for varying vacuum chamber pressures. Right, beam power as a function of vacuum chamber pressure, presented on a semilog scale. Data from DC-ION.

At small increases to neutral density within the discharge chamber, we would expect an increase in double-ionization events: electrons that had previously escaped the collision are more likely to encounter a neutral xenon and, as the presence of ions increases, a singly-ionized xenon ion. As such, examination of the beam current density consisting of double ions can provide additional information on the changes to the thruster operation. Fig. 6 shows the beam double ion current density along the radius, with clear indication of increased double ion production not only near the centerline but along the whole radius of the grid.

Figure x presents the beam power from double ions as a function of vacuum chamber pressure on a semilog scale. As seen with the beam power as a whole, the beam power from double ions increases almost linearly with vacuum chamber pressure.

C. Summary

Using the NSTAR TH15 configuration and several basic assumptions, we modeled beam characteristics as functions of vacuum chamber pressure ranging from 10^{-7} Torr to 10^{-4} Torr and the true vacuum condition (as control/comparative case).

The results indicate a largely linear trend in beam power (both total and from double ions) with increasing vacuum chamber pressure. This is possibly a result of Eq. (3), which presumes a linear flux model for constant chamber pressure

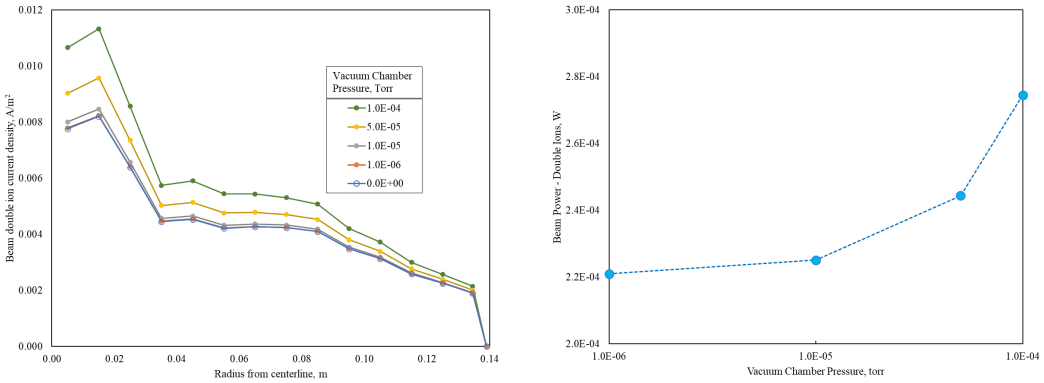

Fig. 6 Left, beam double ion current density along the radius for varying vacuum chamber pressures. Right, beam power from double ions as a function of vacuum chamber pressure, presented on a semilog scale. Data from DC-ION..

and, thus, a linear ingestion factor λ_i for constant $\Gamma_d c$. These results should be compared to actual beam current measurements at various vacuum chamber pressures if such data exists.

The use of a an average grid neutral density and temperature may introduce some approximation. Additional modeling with λ_i (and thus ϕ_p) as functions of the grid radius is planned for the future and well within the capabilities of the current model.

As more complex modeling of Γ_t and Γ_{env} can be achieved, we expect the ingestion factor λ_i will play an increasingly critical role in modeling ingestion.

IV. Compensating for Ingestion

As demonstrated in the prior section, ingestion of neutrals from the vacuum chamber modifies the operation of the thruster. This is observed as an increase in beam power and overall efficiency when compared to true vacuum operation. In order to better leverage in-facility results for thruster design and optimization, it is desirable to somehow compensate for ingestion and return the thruster to more space-like operation.

One reasonable approach is to adjust the flow of propellant into the discharge chamber through the plenum. The ingestion of neutrals through the grid can be interpreted as an increase in propellant flow into the discharge chamber; to compensate for this addition, we would need to reduce the controlled flow by some amount. While a linear adjustment (reducing propellant flow rate by the exact rate of ingestion) would be the most obvious, the complex relationship between neutral density, ion generation, and grid transparency merits a more careful analysis.

A logical assumption is that the adjustment to the propellant flow is some function of the ingestion factor; that is:

$$\frac{\dot{m}_{in,adjusted}}{\dot{m}_{in}} = f(\lambda_i, ...) \tag{27}$$

As an initial approach, assuming $f(\lambda_i, ...)$ is linear to λ_i is the most simple. Given that the ingestion factor λ_i is a relative description of flux into the chamber, compensating for that flux implies a difference, e.g.:

$$\frac{\dot{m}_{in,adjusted}}{\dot{m}_{in}} = (1 - c\lambda_i) \tag{28}$$

... where c is some scaling parameter on λ_i. In terms of the equation, this scaling factor represents the portion of ingested neutrals (λ_i) that, at steady state, remain in the chamber.

Using this function, the most obvious case occurs where c=1, which assumes that all ingested neutrals would remain as neutrals. This is obviously unrealistic, as a portion of neutrals ingested will eventually be subject to ejection as either neutral loss or ions.

Instead, we propose and analyze two methods for determining c and thus the change to flow rate through the plenum.

A. Enforcing Constant Neutral Density

As an initial investigation, we seek to determine c through holding the neutral density within the discharge chamber constant. To do so, we first need to introduce a relationship between our known values for neutral density and propellant flow rate. The standard relationship involves propellant utilization η_p:

$$\eta_p = \frac{\dot{m}_{ions}}{\dot{m}_{in}} \tag{29}$$

... where $\dot{m}_{ions}$ is the flow of ions out of the discharge chamber and $\dot{m}_{in}$ is the propellant flow into the discharge chamber. Propellant utilization represents the portion of propellant that results in useful ions in the beam.

The standard equation for calculating neutral density within a direct current GIT discharge chamber is:

$$n_o = \frac{\dot{m}_{in}(1-\eta_p)\sqrt{8\pi m}}{\phi A_{grid}\sqrt{kT_t}} \tag{30}$$

... where $\dot{m}_{in}$ is in kg/s and all other values are known. For a specific geometry, we can remove the constant factors and thus say that:

$$n_o \propto \frac{\dot{m}_{in}(1-\eta_p)}{\phi\sqrt{T_t}} \tag{31}$$

Equation (31) relates the neutral density within the chamber to propellant flow, propellant utilization, neutral temperature, and grid neutral transparency. Using this, we can equate two operational states of the thruster: the true vacuum condition with transparency ϕ (a) and the derived vacuum condition with pseudo-transparency ϕ_p mimicking ingestion (b). Our goal is to reproduce beam characteristics; to that end, we assume ion flow $\dot{m}_{ions}$ is constant; to generate similar ion flows, we also assume that discharge chamber neutral density n_o and neutral temperature T_o are also constant. We start with the assumption of constant neutral density, allowing us to state:

$$\frac{\dot{m}_{in,a}(1-\eta_{p,a})}{\phi\sqrt{T_{t,a}}} = \frac{\dot{m}_{in,b}(1-\eta_{p,b})}{\phi_p\sqrt{T_{t,b}}} \tag{32}$$

If ion flow is constant, then we can calculate $\eta_{p,b}$ as:

$$\eta_p = \frac{\dot{m}_{ions,b}}{\dot{m}_{in,b}} = \frac{\dot{m}_{ions,a}}{\dot{m}_{in,b}} = \frac{\eta_{p,a}\dot{m}_{in,a}}{\dot{m}_{in,b}} \tag{33}$$

Substituting Eq. (33) into Eq. (32) and assuming $T_{t,a} = T_{t,b}$, we get:

$$\frac{\dot{m}_{in,a}(1-\eta_{p,a})}{\phi} = \frac{\dot{m}_{in,b}(1-\frac{\eta_{p,a}\dot{m}_{in,a}}{\dot{m}_{in,b}})}{\phi_p} \tag{34}$$

$$\frac{\phi_p}{\phi}\dot{m}_{in,a}(1-\eta_{p,a}) = \dot{m}_{in,b} - \eta_{p,a}\dot{m}_{in,a} \tag{35}$$

$$\dot{m}_{in,b} = \frac{\phi_p}{\phi}\dot{m}_{in,a}(1-\eta_{p,a}) + \eta_{p,a}\dot{m}_{in,a} \tag{36}$$

$$\dot{m}_{in,b} = ((1-\lambda_i)(1-\eta_{p,a}) + \eta_{p,a})\dot{m}_{in,a} \tag{37}$$

$$\dot{m}_{in,b} = (1-\eta_{p,a} - \lambda_i(1-\eta_{p,a}) + \eta_{p,a})\dot{m}_{in,a} \tag{38}$$

$$\dot{m}_{in,b} = (1-\lambda_i(1-\eta_{p,a}))\dot{m}_{in,a} \tag{39}$$

This equation, arrived at independently, fits the form of Eq. (28). In this derivation, the value for the scaling factor c is set as $(1-\eta_{p,a})$.

Using Eq. (39), we can calculate a rate of propellant flow in the second case that should compensate for ingestion into the thruster (as represented by ϕ_p) and reproduce the neutral density for the true vacuum case. Propellant flow into the discharge chamber occurs through both plenum and cathode; we choose to hold the flow through the cathode constant, as doing otherwise introduces new variation to the internal state. We thus extend Eq. (39) to determine the plenum flow rate:

$$\dot{m}_{plenum,b} + \dot{m}_{cathode} = (1-\lambda_i(1-\eta_{p,a}))(\dot{m}_{plenum,a} + \dot{m}_{cathode}) \tag{40}$$

$$\dot{m}_{plenum,b} = \dot{m}_{plenum,a} + \dot{m}_{cathode} - \lambda_i(1-\eta_{p,a})(\dot{m}_{plenum,a} + \dot{m}_{cathode}) - \dot{m}_{cathode} \quad (41)$$

$$\dot{m}_{plenum,b} = \dot{m}_{plenum,a} - \lambda_i(1-\eta_{p,a})(\dot{m}_{plenum,a} + \dot{m}_{cathode}) \quad (42)$$

For the true vacuum case as modeled previous (NSTAR TH15), η_p was calculated as 77.7%. With this value and the information in Tables 1 and 2, we can calculate the new plenum flow rate for the specified vacuum chamber conditions.

Table 3 Adjusted plenum flow rate for NSTAR thruster TH15 operation with various vacuum chamber pressures including the default case (pressure = 0 Torr); adjustment based on constant n_t.

Pressure Env Torr given	Ingestion Factor λ_i Eq. (23)	Pseudo-Transparency ϕ_p Eq. (26)	Adjusted Plenum Flow, n_t $\dot{m}_{plenum,b}$ Eq. (42)
0.00	0.000%	15.61%	23.420
$1.00\text{x}10^{-7}$	0.018%	15.61%	23.419
$1.00\text{x}10^{-6}$	0.176%	15.58%	23.409
$1.00\text{x}10^{-5}$	1.765%	15.33%	23.313
$5.00\text{x}10^{-5}$	8.824%	14.23%	22.885
$1.00\text{x}10^{-4}$	17.65%	12.86%	22.350

We modeled thruster beam characteristics using the values in Table 3 to determine the impact relative to the unadjusted (standard) plenum flow rates shown previously. For beam current density, the adjustment lowered the beam current density at all radius locations, shifting the individual profiles closer to the standard true vacuum case (Fig. 7, left; for comparison, see Fig. 5). A presentation of beam power as a function of vacuum chamber density for both the standard plenum flow and the adjusted plenum flow more clearly demonstrates the shift towards the true vacuum case.

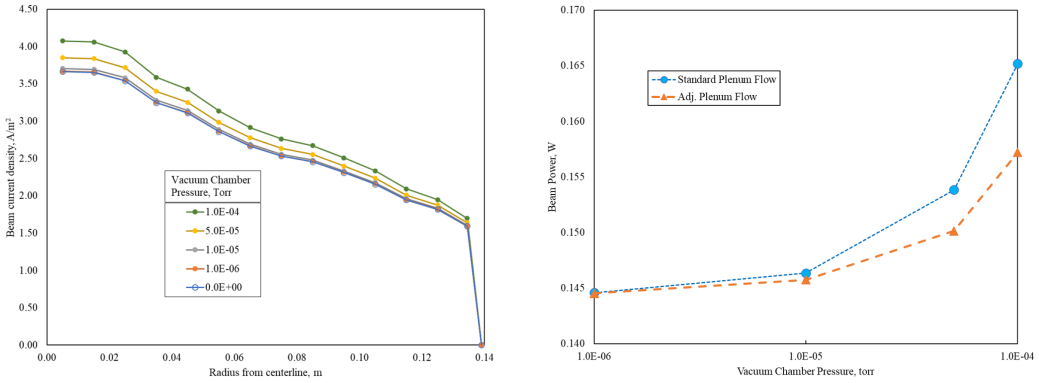

Fig. 7 Left, beam current density along the radius for varying vacuum chamber pressures and with plenum flow adjusted to maintain constant neutral density. Right, beam power as a function of vacuum chamber density on a semilog scale for standard plenum flow and plenum flow adjusted to maintain constant neutral density. Data from DC-ION.

Consistent with the overall beam results are the observed changes in the beam resulting from doubly ionized xenon. The relative changes in both double ion beam current density and double ion beam power match those for overall beam power, indicating that the relationship between beam power and double ionization has not changed for these adjusted cases.

As shown, adjustment of propellant flow using the ingestion factor and a scaling factor of $(1-\eta_p)$ to maintain neutral density between true vacuum and pseudo-transparency (ingestion) cases does produce a beam that is closer to the true vacuum case. This shows that the method of lowering plenum flow to is sound and that the general form for the adjustment based on λ_i is useful, while the exact value of scaling factor needs to be modified. While the adjustment is insufficient overall, the relative decrease in beam power across all vacuum chamber pressures remained consistent, indicating that the adjustment does appear to be linear with the ingestion factor.

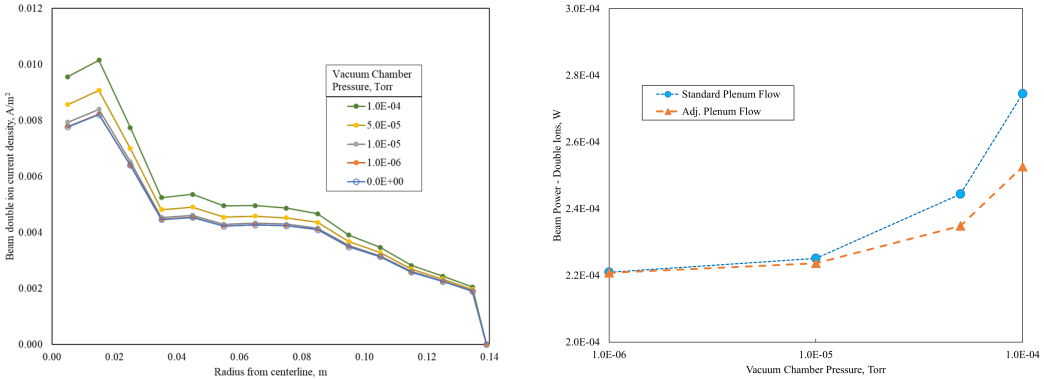

Fig. 8 Left, double ion beam current density along the radius for varying vacuum chamber pressures and with plenum flow adjusted to maintain constant neutral density. Right, double ion beam power as a function of vacuum chamber density on a semilog scale for standard plenum flow and plenum flow adjusted to maintain constant neutral density. Data from DC-ION.

B. Alternative Scaling

In pursuit of a better adjustment to the plenum flow and in light of the relevance of the ingestion factor, we consider in our second case there is a complex interaction within the discharge chamber between propellant flow, neutral density, ion generation, and grid transparency. If we assume ingested gas contributes to neutral density along the grid (as it obviously does), we then must assume that, as thruster operation initiates and the discharge chamber climbs to steady state, some portion of the ingested neutrals will themselves participate in neutral flux back to the grid and, thus, neutral loss. In a rough mathematical form:

$$\dot{m}_{ingested} = \dot{m}_{ingested,lost} + \dot{m}_{ingested,retained} \tag{43}$$

In the previous approach, Eq. (39) effectively sets c equal to $(1-\eta_p)$; this was obviously insufficient to fully compensate for the ingestion, implying that the rate of retention for ingested neutrals is higher than the overall propellant utilization would suggest. Stated differently, a propellant utilization of 77.7% implies that 22.3% of the propellant added will be eventually ejected as neutrals with 77.7% becoming ionized (and, at steady state, escaping); while c=1 would have 100% remain as neutrals on ejection (a value that is certainly too high), the results of modeling would indicate that 22.3% is too low to compensate for the additional pseudo-retention (ingestion).

As an alternative, a simple assumption would be that $\dot{m}_{ingested,lost} = \dot{m}_{ingested,retained}$, so that each represent one half of $\dot{m}_{ingested}$. Thus, we scale our ingestion factor with $c = 0.5$, and our new propellant flow calculation becomes:

$$\dot{m}_{in,b} = (1 - 0.5\lambda_i)\dot{m}_{in,a} \tag{44}$$

Extrapolating to the plenum flow as done previously, we have:

$$\dot{m}_{plenum,b} = \dot{m}_{plenum,a} - 0.5\lambda_i(\dot{m}_{plenum,a} + \dot{m}_{cathode}) \tag{45}$$

This is an obvious approximation; the true weighting in Eq. (43) will likely be more complicated to discern. For demonstration purposes, however, the approximation proves useful. Table 4 has the parameters used for the plenum flow adjustment based on $0.5\lambda_i$.

Modeling with these parameters produces a significant change relative to both the standard (unadjusted) plenum flow and the plenum flow adjusted for constant neutral density. When we compare the beam current density for this new case (Fig. 9), we see that a scaling factor of $c = 0.5$ reduces the beam current density almost to the true vacuum case across the vacuum pressures tested. The righthand image provides more support of this reduction: total beam power for the 10^{-6} Torr and 10^{-5} Torr models are almost equal, while the increased pressure cases show gradual but less severe increases in beam power.

Similarly, comparison of double ion beam power and current density also show significant reduction towards the standard true vacuum case. At the outer third of the thruster grid, which contribute more heavily to total beam power, the double ion current density for all cases is indistinguishable from the standard true vacuum case. Only near the center line does double ion generation increase for the higher pressure cases.

Table 4 Adjusted plenum flow rate for NSTAR thruster TH15 operation with various vacuum chamber pressures including the default case (pressure = 0 Torr); adjustment based on $0.5\lambda_i$.

Pressure Env Torr given	Ingestion Factor λ_i Eq. (23)	Pseudo-Transparency ϕ_p Eq. (26)	Adjusted Plenum Flow, λ_i $\dot{m}_{plenum,b}$ Eq. (45)
0.00	0.000%	15.61%	23.420
$1.00\text{x}10^{-7}$	0.018%	15.61%	23.418
$1.00\text{x}10^{-6}$	0.176%	15.58%	23.396
$1.00\text{x}10^{-5}$	1.765%	15.33%	23.180
$5.00\text{x}10^{-5}$	8.824%	14.23%	22.222
$1.00\text{x}10^{-4}$	17.65%	12.86%	21.024

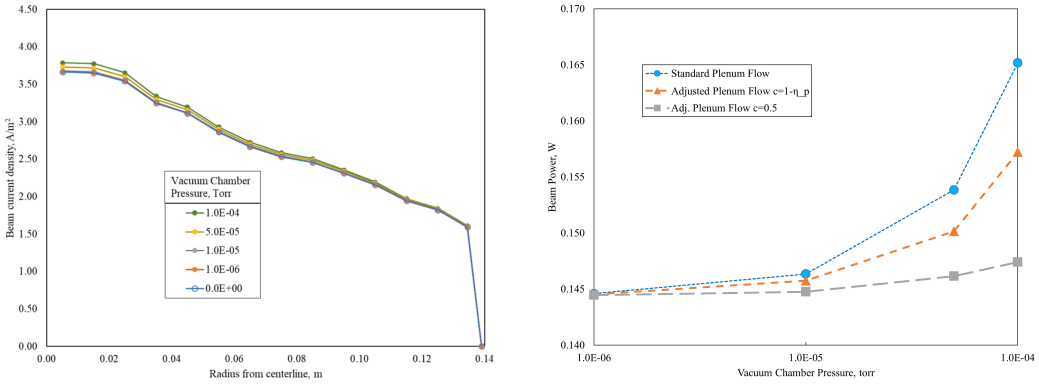

Fig. 9 Left, beam current density along the radius for varying vacuum chamber pressures and with plenum flow adjusted by $c = 0.5$. Right, beam power as a function of vacuum chamber density on a semilog scale for standard plenum flow, plenum flow adjusted $c = 1 - \eta_p$, and plenum flow adjusted by $c = 0.5$. Data from DC-ION.

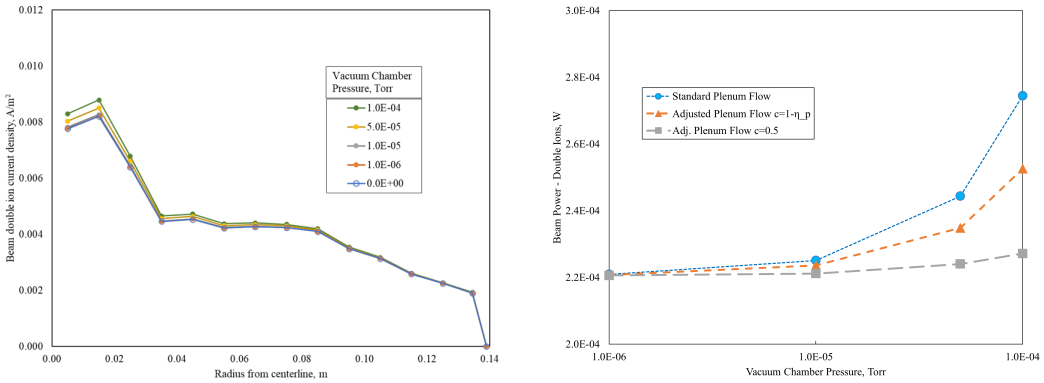

Fig. 10 Left, double ion beam current density along the radius for varying vacuum chamber pressures and with plenum flow adjusted by $c = 0.5$. Right, double ion beam power as a function of vacuum chamber density on a semilog scale for standard plenum flow, plenum flow adjusted $c = 1 - \eta_p$, and plenum flow adjusted by $c = 0.5$. Data from DC-ION.

C. Summary

With the results from modeling pseudo-transparency indicating significant changes to beam power characteristics even at lower vacuum chamber pressures, we approached how to adjust operation of the thruster at each vacuum pressure to compensate for ingestion and better reproduce operation in a true vacuum. To do so, we proposed adjusting propellant flow by some amount, reasoning that ingestion of neutrals could be interpreted as a second (or third) propellant source

in excess of the intended standard propellant flow. We leveraged the ingestion factor λ_i and assumed a linear form of the equation to calculate the adjusted plenum flow, in which a scaling factor c was assumed to operate on the ingestion factor.

We then modeled two distinct methods for determining c. The first method was based on maintaining a constant neutral density within the discharge chamber. Through separate derivation, we arrived at an adjustment function identical to our assumed function but with a specific value of $c = 1 - \eta_{p,a}$, with $\eta_{p,a}$ being the propellant utilization of the thruster in the true vacuum condition. As a result, the function assumes that neutrals ingested from the environment are ionized at the same rate as standard propellant. Modeling the resulting plenum flow rates with the pseudo-transparency rates calculated previously, we observed that beam characteristics shifted closer to the standard true vacuum case. However, the shift was smaller than desired.

In the second method, we assume that neutrals ingested are retained at a much higher rate than the thruster's propellant utilization would suggest (50% versus 22.7% as determined by propellant utilization), thus setting $c = 0.5$. Modeling with this adjustment provided results that were much more in line with the standard true vacuum case: for vacuum chamber pressures below 10^{-5} Torr, the examined beam characteristics were indistinguishable from the true vacuum case, and those at or above 10^{-5} Torr showed only minimal variation.

It is therefore reasonable to state that the general function for propellant flow adjustment as given in Eq. (28) is consistent with modeling for the given parameters and thruster. The ingestion factor proves useful to determining the adjustment needed. Additionally, the desired value for scaling factor c is slightly above 0.5 for these cases; it is likely that other configurations or geometries will result in different scaling factors.

V. Conclusion

To investigate the effects of neutral ingestion on the operation of a gridded ion thruster, we explored a new approach to modeling such ingestion. Using a flux ratio defined as the ingestion factor, we calculated a pseudo-transparency value to reproduce the ingestion of neutrals by reflecting more of the discharge chamber's thrust back into the chamber. Increasing background pressure within the vacuum chamber corresponded to increased ingestion and decreased pseudo-transparency. Modeling the NSTAR thruster at throttle level 15 but with the calculated pseudo-transparency, we observed significant increases in beam current density and beam power even at typical background pressures (10^{-5} Torr).

Following these calculations, we then sought to counter the effects of the simulated ingestion by adjusting plenum flow into the discharge chamber. We defined the modified plenum flow as a function of the ingestion factor and a scaling value c. We then experimented with a derivation based on the thruster's propellant utilization resulting in c=0.223 and a separate set of scenarios with c determined through analytical reasoning as c=0.5. Both cases showed decreases in excess beam characteristics, bringing operation closer to the true vacuum TH15 case; c=0.5, however, proved to be much closer to the desired scaling factor, eliminating almost all of the excess beam power and current density.

These results show that the pseudo-transparency model has potential for use in future facility effect modeling and testing. Future work will include validation against experimental measurements, refinement of analysis to determine the best value of the scaling factor c, and exploring more precise calculations of neutral flux from both the thruster and the environment.

Appendix

Conversion from a given pressure P in Torr to particle density n is accomplished via the ideal gas equation as follows:

$$n = \frac{NN_a}{V} = \frac{P_{Pa}N_A}{RT} \tag{46}$$

... where N is the number of moles of gas, N_A is Avogadro's number, P_{Pa} is the pressure in Pa, V is the volume of gas in m^3, R is the ideal gas constant, and T is the temperature of the gas in Kelvin. We can then convert to P in Torr and simplify as follows:

$$n = \frac{P * 133.32\frac{Pa}{torr} * 6.022x10^{23}mol^{-1}}{8.314\frac{Pa*m^3}{K*mol}T} \tag{47}$$

$$n = 9.6566x10^{24}\frac{P}{T} \tag{48}$$

Acknowledgments

This work was funded by Joint Advanced Propulsion Institute 20-STRI-FULL-0004, NASA Grant Number 80NSSC21K1118.

References

[1] Wirz, R. E., Gorodetsky, A. A., Jorns, B. A., and Walker, M. L. R., "Predictive Engineering Modeling for Life and Performance Assessment of Electric Propulsion Systems," *AIAA SCITECH 2022 Forum*, 2022, p. 410.

[2] Bapat, A., Salunkhe, P. B., and Patil, A. V., "Hall-Effect Thrusters for Deep-Space Missions: A Review," *IEEE Transactions on Plasma Science*, 2022.

[3] Uchizono, N. M., and Wirz, R. E., "Facility Effects for Electrospray Thrusters," *AIAA SCITECH 2022 Forum*, 2022, p. 1361.

[4] Hall, S. J., Gray, T. G., Yim, J. T., Choi, M., Sarver-Verhey, T. R., and Kamhawi, H., "The effect of facility background pressure on hollow cathode operation," *Journal of Applied Physics*, Vol. 130, No. 11, 2021, p. 113302.

[5] Wachs, B., and Jorns, B., "Background pressure effects on ion dynamics in a low-power magnetic nozzle thruster," *Plasma Sources Science and Technology*, Vol. 29, No. 4, 2020, p. 045002.

[6] Jovel, D. R., Nauschütt, B., Walker, M. L., and Klar, P. J., "Facility Effects on Ion Flux Measurements of the Radiofrequency Ion Thruster 10 cm (RIT-10)," 2020.

[7] Frieman, J. D., Liu, T. M., and Walker, M. L., "Background flow model of Hall thruster neutral ingestion," *Journal of Propulsion and Power*, Vol. 33, No. 5, 2017, pp. 1087–1101.

[8] MacDonald-Tenenbaum, N., Pratt, Q., Nakles, M., Pilgram, N., Holmes, M., and Hargus Jr, W., "Background pressure effects on ion velocity distributions in an SPT-100 Hall thruster," *Journal of Propulsion and Power*, Vol. 35, No. 2, 2019, pp. 403–412.

[9] Hall, S. J., Jorns, B. A., Gallimore, A. D., Kamhawi, H., and Huang, W., "Plasma Plume Characterization of a 100 kW Nested Hall Thruster," *Journal of Propulsion and Power*, Vol. 38, No. 1, 2022, pp. 97–110.

[10] Brieda, L., Raitses, Y., Choueiri, E., Myers, R., and Keidar, M., "Quasi-steady testing approach for high-power Hall thrusters," *Journal of Applied Physics*, Vol. 130, No. 18, 2021, p. 183303.

[11] Wirz, R. E., *Discharge plasma processes of ring-cusp ion thrusters*, California Institute of Technology, 2005.

[12] Dankanich, J. W., Walker, M., Swiatek, M. W., and Yim, J. T., "Recommended practice for pressure measurements and calculation of effective pumping speeds during electric propulsion testing," *International Electric Propulsion Conference (IEPC)*, 2013.

[13] Van Noord, J. L., Soulas, G. C., and Sovey, J. S., "NEXT PM1R Ion Thruster and Propellant Management System Wear Test Results," *31st International Electric Propulsion Conference*, 2009, pp. 20–24.